

X-ray flares from propagation instabilities in long Gamma-Ray Burst jets

D. Lazzati¹, C. H. Blackwell¹, B. J. Morsony² and M. C. Begelman^{3,4}

¹*Department of Physics, NC State University, 2401 Stinson Drive, Raleigh, NC 27695-8202*

²*Department of Astronomy, University of Wisconsin-Madison, 5534 Sterling Hall, 475 N. Charter Street, Madison WI 53706-1582*

³*JILA, University of Colorado, 440 UCB, Boulder, CO 80309-0440*

⁴*University of Colorado, Department of Astrophysical and Planetary Sciences, 391 UCB, Boulder, CO 80309-0391*

26 October 2021

ABSTRACT

We present a numerical simulation of a gamma-ray burst jet from a long-lasting engine in the core of a 16 solar mass Wolf-Rayet star. The engine is kept active for 6000 s with a luminosity that decays in time as a power-law with index $-5/3$. Even though there is no short time-scale variability in the injected engine luminosity, we find that the jet’s kinetic luminosity outside the progenitor star is characterized by fluctuations with relatively short time scale. We analyze the temporal characteristics of those fluctuations and we find that they are consistent with the properties of observed flares in X-ray afterglows. The peak to continuum flux ratio of the flares in the simulation is consistent with some, but not all, the observed flares. We propose that propagation instabilities, rather than variability in the engine luminosity, are responsible for the X-ray flares with moderate contrast. Strong flares such as the one detected in GRB 050502B, instead, cannot be reproduced by this model and require strong variability in the engine activity.

Key words: gamma-ray burst: general — radiation mechanisms: non-thermal

1 INTRODUCTION

One of the most surprising discoveries of the Swift satellite has been the presence, in approximately 30 per cent of the X-ray afterglows, of flaring activity on top of the smooth afterglow decay (Burrows et al. 2005; Falcone et al. 2006, 2007; Nousek 2006; Chincarini et al. 2007, 2010, Margutti et al. 2010b). The temporal properties of the flares, and especially the fact that they have a duration that is shorter than the time at which they appear in the light curve, have lead to the conclusion that the flares’ most likely origin is late-time activity of the inner engine (Ioka et al. 2005; Zhang et al. 2006; Lazzati & Perna 2007, Curran et al. 2008). As a matter of fact, any disturbance in the brightness that takes place simultaneously on the surface of a spherical relativistic fireball produces a flare whose duration is at least equal to the time of the peak (see, however, Giannios 2006 for a model of magnetic dissipation on the external shock). In addition, X-ray flares show spectral and temporal properties similar to the prompt emission of GRBs (Margutti et al. 2010a).

The inner engine of GRBs therefore has to be active, at least in some cases, for a time much larger than the few hundreds of seconds of the duration of the prompt emission (Kouveliotou et al. 1993). The mechanism that keeps the engine alive and the mechanism for the production of the flares are, however, still matter of active debate. In the

collapsar scenario (Woosley 1993), the reason for the continued activity of the engine is either fall-back material from the exploding star (Chevalier 1986; MacFadyen et al. 2001; Zhang & Woosley 2008) or the disk itself that takes some time to accrete all its matter (Cannizzo et al. 1990). In the magnetar model (e.g. Usov 1992; Bucciantini et al. 2008), on the other hand, the engine activity is due to the continuous spin-down of the neutron star. What is unclear, for any choice of the inner engine, is the source of the intermittent behavior of the flaring activity. While during the prompt phase the engine is active for most of the time, during the flaring phase the engine is mostly inactive.

Until now, models had concentrated on finding a source of variability that is intrinsic to the engine, i.e., the engine itself releases energy in a flaring fashion. Perna et al. (2006) proposed gravitational instability in the outer parts of the accretion disk as the source of the flare intermittent behavior (see also Proga & Zhang 2006; Piro & Pfahl 2007). Lazzati et al. (2008) proposed that the switch from a neutrino cooled thin disk to a thick disk could be the reason for the change in behavior. In this paper, we show that even if the inner engine is continuous with a featureless power-law decay, the jet interaction with the disrupting star brings about variations in the jet energy that resemble in luminosity and temporal evolution the properties of the observed flares.

arXiv:1008.4364v2 [astro-ph.HE] 16 Nov 2010

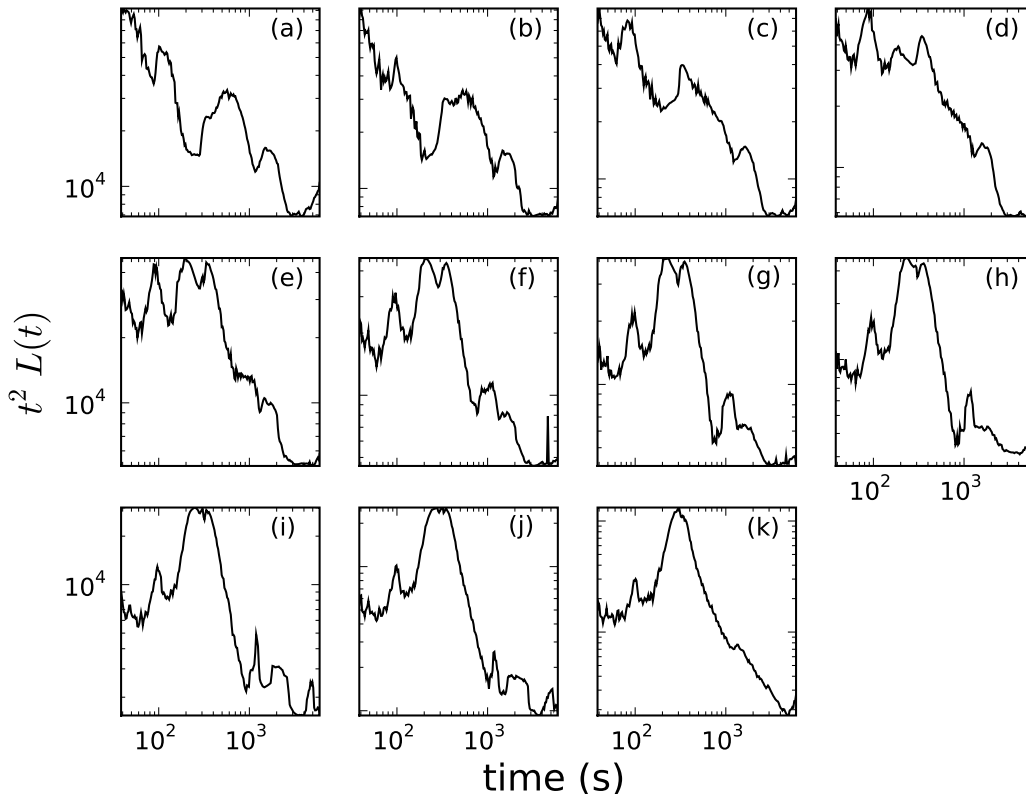


Figure 1. Light-power curves derived from our numerical simulation. Light-power curves were calculated for observers lying at viewing angles of 1, 2, 3, 4, 5, 6, 7, 8, 9, 10, and 16 degrees from the jet axis [panels (a) through (k)]. All the light-power curves are multiplied by t^2 to enhance the presence of flares on top of the overall decay behavior.

This paper is organized as follows: in Sect. 2 we describe our numerical simulation and how we derived light curves, in Sect. 3 we discuss the characterization of the flares and the results, in Sect. 4 we discuss a physical mechanism for the fluctuations, and in Sect. 5 we discuss and summarize our findings.

2 NUMERICAL SIMULATION AND LIGHT-POWER CURVES

This paper is based on the results of a numerical simulation of a GRB progenitor with a central engine that stays active for a long time. The progenitor star used in the simulation was model 16TI from Woosley & Heger (2006), a 16 solar masses Wolf-Rayet star evolved to pre-explosion. This progenitor is the same used in previous simulations from our group (Morsony et al. 2007, 2010; Lazzati et al. 2009, 2010). The jet was injected as a boundary condition with an opening angle $\theta_0 = 10^\circ$, a Lorentz factor $\Gamma_0 = 5$ and internal energy sufficient to reach an asymptotic Lorentz factor $\Gamma_\infty = 400$, in case of full, non-dissipative acceleration. The jet luminosity was initially set to constant $L_0 = 5.33 \times 10^{50}$ erg s $^{-1}$. At 7.5 s after the ignition the luminosity was changed into a smoothly decaying power-law $L(t) = L_0(t/7.5)^{-5/3}$, where the exponent was chosen to

mimic the accretion rate of fall-back material¹ (Chevalier 1989; MacFadyen et al. 2001). The engine was turned off at 6000 s after ignition, at which time the simulation was also stopped. The simulation was performed with the adaptive mesh refinement code FLASH (Fryxell et al. 2000) with resolution and refinement scheme analogous to Morsony et al. (2007).

Our simulation has two major limitations that were made necessary by technical limitations and by the need of simplifying the setup in order to be able to extend the engine life-time maintaining the overall run time reasonable. First, even though we mention fallback accretion as a possible source of the extended energy release from the inner engine, we do not simulate the actual fall-back inflow. Second, our simulation does not include magnetic fields, given the technical difficulty of performing special-relativistic magneto-hydrodynamic simulations with an adaptive mesh refinement scheme. Despite these two limitations we believe that our simulations give a credible description of the jet-star interaction. The fall-back inflow should not affect the jet

¹ Note that the assumption of a linear relation between accretion rate and outflow luminosity is appropriate for magnetic jet driving (e.g. Barkov & Komissarov 2010) while a steeper relation should be used in case of a neutrino driven outflow ($L_{\text{jet}} \propto \dot{m}^{9/4}$, Zalamea & Beloborodov 2010).

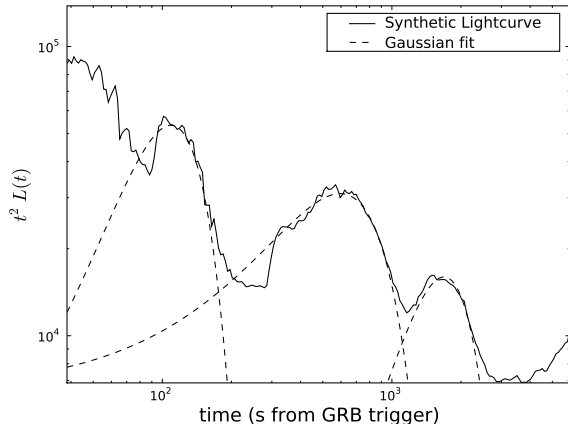


Figure 2. A sample light curve (for an observer at $\theta = 1^\circ$), with best fit Gaussian functions overlaid on the identified flares.

dynamics in our computation box both because we do not simulate the inner core of the star and because the inflow is expected to be more relevant in the equatorial area. The effect of the lack of magnetic fields is more difficult to evaluate. As a matter of fact, it is very likely that the jet is launched by a magnetic mechanism, especially during the low-luminosity phase when the neutrino cooling has been switched-off. The subsequent evolution of the jet during the acceleration phase decreases the magnetization and, at the radii of the outer boundary of our computational box, it is likely that the jet is already matter dominated (Tchekhovskoy et al. 2010). Hopefully special relativistic MHD simulations with a similar setup will become feasible in the near future to confirm the details of our results.

The simulation was analyzed to derive light-power curves as described in Morsony et al. (2010). Light-power curves are proxies to the light curves that can be computed from simulations that do not extend in radius far enough to allow for the direct comparison of the light curve. Light-power curves assume that the efficiency of conversion of energy into radiation is constant. Light-power curves are not sensitive to spectral evolution, and are therefore a proxy to the bolometric light curve and not to the light curve in a particular band. The light-power curves for observers at angles of 1, 2, 3, 4, 5, 6, 7, 8, 9, 10, and 16 degrees were calculated, including only material with an asymptotic Lorentz factor of at least 10. Light-power curves were extracted at a radius of 2.5×10^{11} cm, close to the outer boundary of our simulation.

3 DATA ANALYSIS AND RESULTS

The light-power curves obtained from the simulation are shown in Figure 1, with the luminosity multiplied by a factor t^2 to emphasize the presence of bumps, the candidate flares. A first finding of our simulation is that the light-power curves decay in time faster than the injected $t^{-5/3}$. This is a consequence of the increase in the opening angle of the jet as the confining power of the progenitor star wanes (Lazzati & Begelman 2005; Morsony et al. 2007). We

find that the slope in the time interval $200 < t < 1000$ s, when the opening angle is growing, is roughly $L(t) \propto T^{-2.4}$, flattening to roughly t^{-2} at later time, when the opening angle enters an almost constant phase. This is an important finding because it highlights the fact that the steep slopes found in the average flare luminosity ($t^{-1.5}$, Lazzati et al. 2008; or even $t^{-2.7}$, Margutti et al. 2010b) may not reflect directly the behavior of the inner engine, and a flatter input is required to reproduce the observations. It is worth emphasizing here that the opening angle $\theta_{\text{sat}} \sim 10^\circ$ at which the increase stops, and consequently the time at which the decay flattens, is dictated by the input opening angle of the simulation ($\theta_0 \sim \theta_{\text{sat}}$) and therefore we do not expect that either the limiting opening angle or the time at which the flattening is observed should be universal among GRBs.

In order to find and characterize the flares that are present in the light-power curves we first subtracted a broken power-law continuum. Typically the subtracted background had a steep early phase and a flatter final, as discussed above for the overall light-power curves. Flares were identified as positive fluctuations in the flux of the background-subtracted curve and characterized by fitting a Gaussian profile letting the peak time, normalization, and width of the Gaussian free to vary. The fits were performed by minimizing the χ^2 statistics, assuming a uniform uncertainty in the data (see Figure 2 for a flare fitting example). Gaussian functions were used in order to make our results directly comparable to the observational results of Chincarini et al. (2007). For the identified flares the ratio of the flare peak flux to the continuum flux under the flare was also evaluated. It is worth noticing that this ratio is an upper limit to what actual observations would provide because we do not have any external shock component in our calculation (see also Section 4).

The results of the flares characterization are shown in Figure 3 and Figure 4. The simulation flares are characterized by a duration that is smaller than their peak time, as found in observational surveys (Chincarini et al. 2007, 2010). In addition, the flare duration is correlated to the flare peak time, another observational finding (see Fig. 10 of Chincarini et al. 2007). The typical flare contrast is of the order of a few, comparable to what found by Chincarini et al. (2007, 2010) and Margutti et al. (2010b). However, our simulation was unable to reproduce the rare but very bright flares observed in some Swift GRBs, with peak flux contrasts up to a hundred or even a thousand.

4 ANALYTICAL MODEL

The simulation that we have presented shows that flaring activity with the temporal characteristics observed in Swift light curves can be reproduced in a simulation with a long-lasting engine that does not have any intrinsic flaring behavior. The origin of the flares lies therefore in propagation instabilities within the jet.

Any variation of the jet luminosity should be accompanied by a variation in the jet opening angle. During the hot phase of the jet, when the jet pressure is high, an increase of the jet luminosity² should be accompanied by an increase

² Note that the jet luminosity can temporally increase even if the

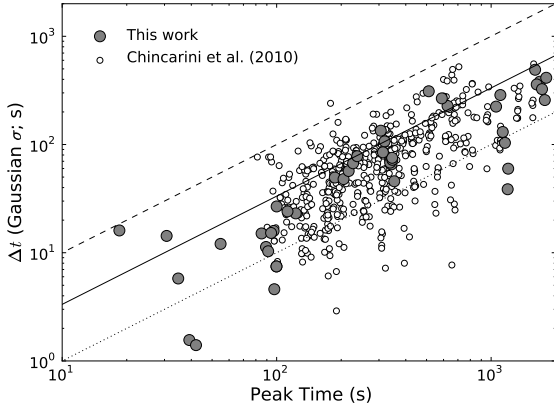


Figure 3. Results of the flare characterization from the synthetic light-power curves in the $(t, \Delta t)$ plane. Each gray dot represents the Gaussian width and peak time of one identified flare. Open, smaller circles are the results of Swift X-ray flares characterization by Chincarini et al. (2010). The dashed, solid, and dotted lines represent the three levels $\Delta t/t = 1, 0.3$, and 0.1 , respectively.

of the opening angle, since the confining pressure of the star is uniform and the increased jet pressure would cause an increase of the opening angle. On the other hand, during the cold phase of the jet, a reduction of the opening angle would bring about an increase of the jet luminosity (at least the specific luminosity per unit solid angle that is responsible for the observed light curve). We therefore expect that early flares are accompanied by an opening angle increase while late flares are simultaneous to a shrinking of the opening angle. This, at least, should be true for the inner parts of the jet. For lines of sight that are close to the edge of the jet, another important factor is whether or not the jet opening angle crosses the line of sight. If the jet opening angle grows to include a particular line of sight, the corresponding light-power curve will show a prominent bump, while a depression would be seen if the jet opening angle decreases. Light curves for observers close to the jet axis and observers close to the jet edge could therefore be anti-correlated. An example of this behavior is the depression observed at $T \sim 200$ s in panels (a), (b), and (c) of Figure 1 (viewing angles of 1, 2, and 3 degrees). At the same time, a bump is seen in panels (e), (f), and (g), for viewing angles of 5, 6, and 7 degrees.

To check for this occurrence, we have calculated the opening angle of the jet to see if there are any variations of the jet opening angle in coincidence with flares in the light curve. The result of this analysis is shown in Figure 5 for the light-power curve calculated at 1° off-axis. There are four prominent flares in the curve and they have been identified with numbers 1, 2, 3, and 4. The comparison indeed reveals that early flares (1 and 2) are accompanied by humps in the opening angle plot, while the late flare (4) is accompanied by a depression. Flare 3 is difficult to evaluate, since it lays on top of an overall growth of the opening angle of the jet.

The duration of flares that are accompanied by a vari-

engine luminosity decreases. For example, a slower outflow ahead of a faster portion of the jet produces a pile-up of jet material that locally increases the jet luminosity without the need of an increase of the engine luminosity.

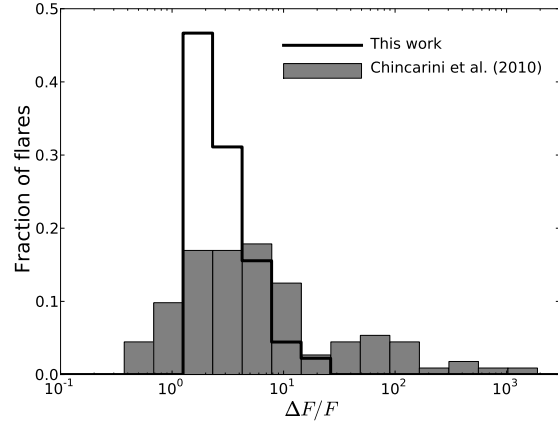


Figure 4. Histogram of the flare contrast from our simulation (thick solid line) compared to observations (shaded area).

ation in the jet opening angle can be computed assuming that the mechanisms that activates and quenches them is the pressure of the surrounding stellar material. In that case, the time it takes for the opening angle to vary can be computed by knowing the jet transverse size and the sound speed in the exploding stellar material.

The time to restore the jet opening angle after a factor of 2 increase in kinetic luminosity (a $\sqrt{2}$ variation in opening angle) would be

$$\delta t \simeq \frac{R_\perp}{3v_s} \simeq \frac{R_* \theta_j}{3v_s} \quad (1)$$

where R_\perp is the jet transverse radius, v_s is the sound speed of the exploding star, R_* is the stellar radius, and θ_j is the jet opening angle. The sound speed of the star is:

$$v_s \simeq \sqrt{\frac{kT_*}{m_p}} \quad (2)$$

where T_* is the average temperature of the star's material and m_p is the proton mass. The temperature of the exploding star can be calculated assuming that the expansion is adiabatic and at constant speed as:

$$T_* \simeq \frac{T_0 R_*^2}{(v_{ej} t)^2} \quad (3)$$

where T_0 is the average stellar temperature immediately after the explosion and v_{ej} the average ejecta radial velocity. These two quantities can be calculated as

$$T_0 \simeq \frac{2Em_p}{3kM_*} \quad (4)$$

and

$$v_{ej} \simeq \sqrt{\frac{2E}{M_*}} \quad (5)$$

where M_* is the stellar mass and we have assumed that all the explosive energy (E) goes into thermal motions (for Eq. 4) or expansion velocity (for Eq. 5). Combining all the above equations, one can find a very simple solution for the typical flare duration:

$$\frac{\delta t}{t} \simeq \frac{\sqrt{3}}{3} \theta \sim 0.1 \quad (6)$$

An important property of Eq. 6 is that all the dependence

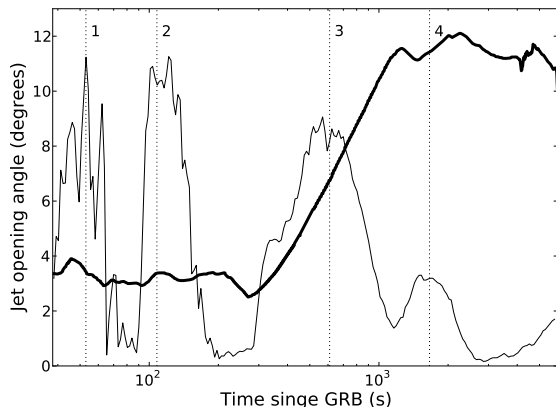


Figure 5. Comparison between the jet opening angle at $R = 2.5 \times 10^{11}$ cm (thick solid line) and the background subtracted light-power curve at $\theta = 1^\circ$ (thin solid line). Prominent flares in the light-power curve have been highlighted with vertical dotted lines and identified with numbers 1, 2, 3, and 4.

on the star property and explosive energy simplify, leaving the opening angle of the jet as the only quantity that can alter the typical flare duration. This simple model reproduces therefore two fundamental properties of the observations: the fact that the flare lasts less than the time at which it peaks and the fact that the flare duration correlates linearly with the peak time.

5 DISCUSSION AND CONCLUSIONS

In summary, the flares that we observe in our simulation are due to two different mechanisms. Early flares, when the jet propagation through the star still excites turbulent motions (Morsony et al. 2007; Mizuta et al. 2010), are due to velocity stratification within the jet, and are accompanied by increases in the opening angle due to the increased jet pressure. Late flares, instead, are due to reductions in the jet opening angle. In both cases, as shown above, the flare duration is smaller than but correlated to the flare peak time.

Even though our simulation shows flares with characteristics that are similar to those observed, it does not show any strong flare with flux contrast larger than about an order of magnitude. Extreme flares with contrast of two or even three orders of magnitude have been observed (Chincarini et al. 2010). Margutti et al. (2010b) show that the distribution of flare contrasts is bimodal and two populations of flares are present. The propagation instabilities that we present here seem to be able to account for the small flares of the main peak (see Figure 4 and Figure 7 in Margutti et al. 2010b). More prominent flares likely require flaring activity in the central engine.

In addition to prominent flares in long-duration GRB afterglows, our model cannot explain the presence of flares in the X-ray afterglows of short-duration GRBs (e.g. Campana et al. 2006). Such flares need therefore a source of variability in the inner engine, such as the disk instability proposed by Perna et al. (2006). Our prediction is therefore that the contrast distribution of short-duration GRB flares should be

analogous to the one of the brighter flares observed in long-duration GRBs. Unfortunately, the flare sample from short GRB afterglows is small and a quantitative comparison is not possible, at this stage.

Another important finding of our simulation is that during the early phases (roughly between few hundreds and one thousand seconds) the light-power curve decay is much steeper than the input luminosity. This is due to the fact that the opening angle of the jet is increasing in that time span, causing the energy to be distributed over a wider portion of the sky. Since the flares follow the light-power curve behavior, the average flare luminosity (Lazzati et al. 2008; Margutti et al. 2010b) also appears to be steeper than what its source mechanism, without the spreading of the opening angle, would produce. In this light, caution must be spent to interpret the steep slopes measured in the average flare light curve since they may be due to much shallower input luminosities. It is tantalizing that Margutti et al. (2010) find a prominent flattening in the average flare light curve at about 1000 s, right when the opening angle of the jet stops growing in our simulation (even though, as mentioned before, the time of the flattening in the simulation is dictated by the input opening angle θ_0 and by the evolution of the jet luminosity. With a constant luminosity of the jet Morsony et al. 2010 find that the opening angle saturates much earlier at $t \sim 50$ s). Unfortunately, however, Margutti et al. (2010) also found that flares at times larger than 1000 s are harder to robustly characterize and their results should be taken with caution at long times.

Finally, we would like to point out that our light-power curves do not include any external shock component. Our flares are therefore likely to be diluted by the synchrotron emission of the external shock. A prediction of our model is therefore that the afterglows dominated by the central engine (Ghisellini et al. 2009) should display stronger flaring activity with respect to afterglow dominated by the external shock component. An indication of this behavior is the decreased occurrence of flares in simple afterglow with no breaks (see Fig. 16 of Margutti et al. 2010a). A word of caution should also be spent for the fact that our light-power curves are calculated at a distance of 2.5×10^{11} cm from the progenitor, close to the outer boundary of our simulation. In reality, the radiation can only be released at the jet photosphere or further out, at a distance at least one order of magnitude larger than our extraction radius. It is possible that the temporal structure of the flares is modified during the further expansion of the jet making the flares longer in time and increasing their $\Delta t/t$. Unfortunately, running a simulation for such a long time (6000 s) forced us to use a relatively small box and made it impossible to perform a fully self consistent calculation with an extraction radius at the jet photosphere or beyond.

6 ACKNOWLEDGMENTS

We would like to thank Guido Chincarini and Raffaella Margutti for kindly making their data available to us. This work was supported in part by NASA ATP grant NNG06GI06G and Swift GI grant NNX08BA92G and by the North Carolina State University Office of Undergraduate Research.

REFERENCES

- Barkov M. V., Komissarov, S. S., 2010, *MNRAS*, 401, 1644
- Bucciantini N., Quataert E., Arons J., Metzger B. D., Thompson T. A., 2008, *MNRAS*, 383, L25
- Burrows D. N., et al., 2005, *Science*, 309, 1833
- Campana S., et al., 2006, *A&A*, 454, 113
- Cannizzo J. K., Lee H. M., Goodman J., 1990, *ApJ*, 351, 38
- Chevalier R. A., 1989, *ApJ*, 346, 847
- Chincarini G., et al., 2007, *ApJ*, 671, 1903
- Chincarini G., et al., 2010, *MNRAS*, 406, 2113
- Curran P. A., Starling R. L. C., O'Brien P. T., Godet O., van der Horst A. J., Wijers R. A. M. J., 2008, *A&A*, 487, 533
- Falcone A. D., et al., 2006, *ApJ*, 641, 1010
- Falcone A. D., et al., 2007, *ApJ*, 671, 1921
- Fryxell B., et al., 2000, *ApJS*, 131, 273
- Ghisellini G., Nardini M., Ghirlanda G., Celotti A., 2009, *MNRAS*, 393, 253
- Giannios D., 2006, *A&A*, 455, L5
- Ioka K., Kobayashi S., Zhang B., 2005, *ApJ*, 631, 429
- Kouveliotou C., Meegan C. A., Fishman G. J., Bhat N. P., Briggs M. S., Koshut T. M., Paciesas W. S., Pendleton G. N., 1993, *ApJ*, 413, L101
- Lazzati D., Begelman M. C., 2005, *ApJ*, 629, 903
- Lazzati D., Perna R., 2007, *MNRAS*, 375, L46
- Lazzati D., Perna R., Begelman M. C., 2008, *MNRAS*, 388, L15
- Lazzati D., Morsony B. J., Begelman M. C., 2009, *ApJ*, 700, L47
- Lazzati D., Morsony B. J., Begelman M. C., 2010, *ApJ*, 717, 239
- MacFadyen A. I., Woosley S. E., Heger, A., 2001, *ApJ*, 550, 410
- Margutti R., Guidorzi C., Chincarini G., Bernardini M. G., Genet F., Mao J., Pasotti F., 2010a, *MNRAS*, 406, 2149
- Margutti A., et al., 2010b, *MNRAS* in press
- Mizuta A., Kino M., Nagakura H., 2010, *ApJ*, 709, L83
- Morsony B. J., Lazzati D., Begelman M. C., 2007, *ApJ*, 665, 569
- Morsony B. J., Lazzati D., Begelman M. C., 2010, submitted to *ApJ* (arXiv:1002.0361)
- Nousek J. A., et al., 2006, *ApJ*, 642, 389
- Perna R., Armitage P. J., Zhang B., 2006, *ApJ*, 636, L29
- Piro A. L., Pfahl E., 2007, *ApJ*, 658, 1173
- Proga D., Zhang B., 2006, *MNRAS*, 370, L61
- Usov V. V., 1992, *Nature*, 357, 472
- Woosley S. E., 1993, *ApJ*, 405, 273
- Woosley S. E., Heger A., 2006, *ApJ*, 637, 914
- Zalamea I., Beloborodov A. M., 2010, *MNRAS* in press (arXiv:1003.0710v3)
- Zhang B., Fan Y. Z., Dyks J., Kobayashi S., Mészáros P., Burrows D. N., Nousek J. A., Gehrels N., 2006, *ApJ*, 642, 354
- Zhang W., Woosley S. E., Heger A., 2008, *ApJ*, 679, 639